

Original citation:

Kleijn, Steven E. F., Lai, Stanley C. S., Miller, Thomas S., Yanson, Alexei I., Koper, Marc T. M. and Unwin, Patrick R.. (2012) Landing and catalytic characterization of individual nanoparticles on electrode surfaces. *Journal of the American Chemical Society*, Volume 134 (Number 45). pp. 18558-18561. ISSN 0002-7863

Permanent WRAP url:

<http://wrap.warwick.ac.uk/54241/>

Copyright and reuse:

The Warwick Research Archive Portal (WRAP) makes the work of researchers of the University of Warwick available open access under the following conditions. Copyright © and all moral rights to the version of the paper presented here belong to the individual author(s) and/or other copyright owners. To the extent reasonable and practicable the material made available in WRAP has been checked for eligibility before being made available.

Copies of full items can be used for personal research or study, educational, or not-for-profit purposes without prior permission or charge. Provided that the authors, title and full bibliographic details are credited, a hyperlink and/or URL is given for the original metadata page and the content is not changed in any way.

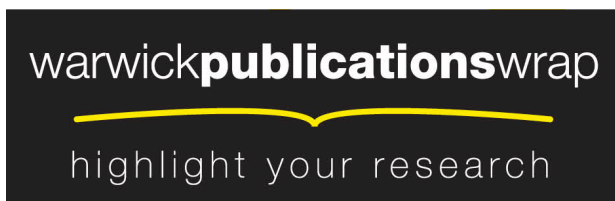
Publisher's statement:

This document is the unedited Author's version of a Submitted Work that was subsequently accepted for publication in *Journal of the American Chemical Society*, © American Chemical Society after peer review. To access the final edited and published work see <http://dx.doi.org/10.1021/ja309220m>

A note on versions:

The version presented here may differ from the published version or, version of record, if you wish to cite this item you are advised to consult the publisher's version. Please see the 'permanent WRAP url' above for details on accessing the published version and note that access may require a subscription.

For more information, please contact the WRAP Team at: wrap@warwick.ac.uk



Landing and Catalytic Characterization of Individual Nanoparticles on Electrode Surfaces

Steven E.F. Kleijn^{‡,†}, Stanley C.S. Lai^{‡,§}, Thomas S. Miller[§], Alexei I. Yanson[†], Marc T.M. Koper^{*,†}, and Patrick R. Unwin^{*,§}

[†] Leiden Institute of Chemistry, Leiden University, PO Box 9502, 2300 RA, Leiden, The Netherlands

[§] Department of Chemistry, University of Warwick, Coventry, CV4 7AL, United Kingdom

Supporting Information Placeholder

ABSTRACT: We demonstrate a novel and versatile pipet-based approach to study the landing of individual nanoparticles (NPs) on various electrode materials, without any need for encapsulation or fabrication of complex substrate electrode structures, providing great flexibility with respect to electrode materials. Due to the small electrode areas defined by the pipet dimensions, the background current is low, allowing for the detection of minute current signals with good time resolution. This approach was used to characterize the potential-dependent activity of Au NPs and to measure the catalytic activity of a single NP on a TEM grid, combining electrochemical and physical characterization at the single NP level for the first time. Such measurements open up the possibility of studying the relation between size and activity of catalyst particles unambiguously.

Metal nanoparticles (NPs) have been extensively studied as electrocatalysts in numerous fields and applications.¹ A key aspect of NPs is their size- and structure-dependent reactivity,^{1c} which is often inferred from ‘top-down’ studies of ensembles of catalytic NPs. However, due to the inherent variance in NP size and shape, only average reactivity trends may be obtained in this way. Even when one can work with a narrow size distribution, subtle effects may substantially alter reactivity. Indeed, we have shown in a previous study that ostensibly similar NPs can have very different reactivity due to subtle variations in morphology.² Therefore, to truly understand NP reactivity on a fundamental level, it is imperative to study single NPs. While such an investigation is demanding, as it requires placing, locating and characterizing a single NP, a few experimental studies have been reported.²⁻³ Single NP studies are further challenging due to the need for high accuracy measurement of the small (current) signals with reasonable bandwidth.^{3h,4}

A recent innovative method to electrochemically detect individual NPs^{3a-f} focuses on NPs that are dispersed in an electrolyte solution, that can diffuse to, and land on, an electrode surface held at a potential where a reaction occurs on the catalytic NP but not on the inert collector electrode. Consequently, arrival of a NP at the electrode surface results

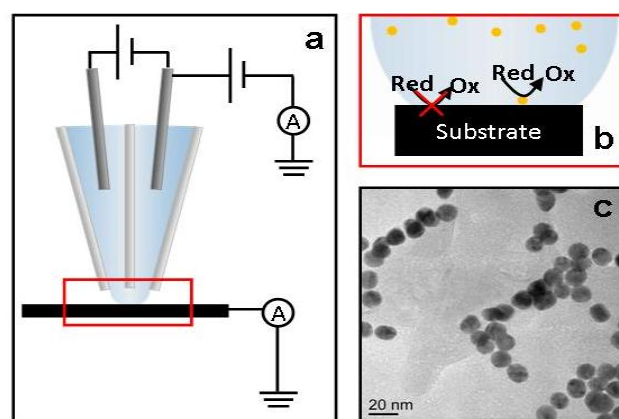


Figure 1 (a) Schematic of the experimental setup. (b) Schematic of the liquid meniscus constituting the electrochemical cell. The substrate is held at a potential where a reaction occurs on the catalytic AuNP, but not on the collector electrode. (c) TEM image of the AuNPs used in this study.

in an increase in current due to the NP reaction, which can be a reaction of a species in solution^{3a} or the oxidation of the NP itself.^{3d} In order to limit the number of NPs landing and minimize the background current, a collector electrode of small area is needed. The preparation of such ultra-microelectrodes (UMEs) greatly limits the choices of substrate material, since not every material (particularly material of practical importance) can be shaped to micro- or nanoscale dimension, and even when the material can be encapsulated, electrode preparation requires considerable time and effort.⁵ A typical UME (~5 μm diameter) often still shows a considerable background signal compared to the electrochemical signal from the NP reaction.^{3a-f} Consequently, only large current signals (often resulting from mass transport limited reactions)^{3a,b} can be detected, and obtaining an entire current-voltage response at an individual NP has so far proved impossible. Furthermore, subsequent characterization of immobilized NPs has proven very challenging.^{5b}

In this paper, we demonstrate the study of single NP reactivity by employing scanning electrochemical cell microscopy (SECCM) to select and isolate a small area on a collector electrode, of any kind of material, and to land, detect and

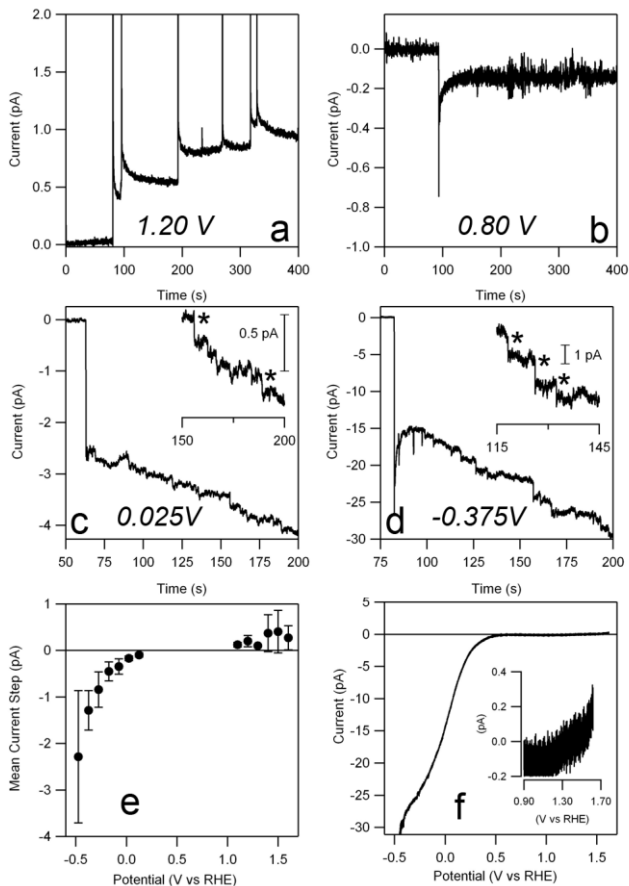


Figure 2 (a-d) Current-time plots showing the landing of the pipet meniscus (initial spike) and AuNPs (subsequent steps) at selected potentials. The current steps in the insets of (c) and (d) are marked (*). (e) Mean current step height determined as a function of substrate potential. Error bars denote 2σ . (f) Linear sweep voltammogram (50 mV s^{-1}) of Au in 5 mM phosphate buffer, measured using a pipet of $1.5 \mu\text{m}$ diameter.

characterize individual NPs. The experimental set-up is schematically depicted in Figure 1a and b and described in full in the Supporting Information. In short, a dual-channel (theta) pipet with a sharp point of approximately $1.5 \mu\text{m}$ diameter was filled with an electrolyte solution of interest (containing $\sim 70 \text{ pM}$ citrate-capped gold NPs (AuNPs), 10-20 nm diameter,⁶ Figure 1c) and two palladium-hydrogen (Pd-H_2 ; $E^0 = 50 \text{ mV}$ vs. reversible hydrogen electrode, RHE)² quasi-reference counter electrodes (QRCEs), both held at the same potential. All potentials throughout this study are reported relative to the RHE. While, in principle, a single barrel pipet could be used, a theta pipet allowed us to monitor the size of the liquid meniscus formed at the end of the pipet by measuring the ionic current between the two QRCEs across the meniscus when a small potential bias was applied, minimizing variability between experiments. Furthermore, the migration rate of charged species can be controlled by the bias potential applied between the QRCEs,⁷ but this option was not employed in this work. The pipet was mounted on a piezoelectric positioning system and slowly lowered towards the substrate, which was held at ground, while the current flowing through the substrate was monitored continuously. Upon contact of the liquid meniscus at the end of the pipet with the substrate, a current spike was observed at the substrate due to the formation of the electrical double layer. This was used to automatically halt the approach so that the pipet was held in place for the duration of the experiment. The resulting meniscus between the pipet and substrate constitutes a micro- or nanoscopic electrochemical cell with the wetted area of the sub-

strate as working electrode, which experiences a potential of the same magnitude but opposite sign as the potential applied to the QRCEs. In this approach, we isolate an area on the working electrode by limiting the electrolyte contact (rather than by decreasing the size of the working electrode, as in previous studies^{3a-f}), which results in at least three main advantages. First, this allows the use of a wide range of electrode materials, size and morphologies, as no traditional UME manufacture is required, instead relying on facile micro- or nanopipet preparation. Second, we can make and break the cell at will on a specific site on the electrode surface (on a millisecond timescale if needed), by simply moving the pipet away from or towards the substrate. This is particularly beneficial if one wishes to land single NPs in a predetermined pattern. Finally, the working electrode area in this pipet-based approach is determined by the size of the pipet,⁷⁻⁸ which can be routinely prepared to be smaller than a typical UME (of several micrometers in diameter), down to $<200 \text{ nm}$.⁹ Such ultra-small surface areas result in a significant decrease in background current (by two orders of magnitude) compared to the UMEs presently used, allowing detection of much smaller currents from the NP reaction itself.

To demonstrate the flexibility of the pipet-based approach, we have landed AuNPs from an aerated 5 mM phosphate buffer solution (pH 7.2) on highly oriented pyrolytic graphite (HOPG) at various potentials. HOPG is an interesting substrate as it serves as a model for novel sp^2 carbon materials and there has been recent debate on the active sites for electron transfer.⁸ Furthermore, the surface of HOPG is easily refreshed (through cleaving with adhesive tape) and has low background currents, making it an attractive collector electrode for NP landing experiments.

Typical current-time plots obtained for the landing of AuNPs on HOPG at various potentials (Figure 2a-d) show a few general trends. Initially, as the pipet is suspended in air, the recorded substrate current is zero. Once the liquid meniscus is brought into contact with the substrate, the electronic circuit is closed, leading to an initial current spike at all potentials (e.g. at $\sim 90 \text{ s}$ in Figure 2a). This current spike can be attributed to the formation of the electric double layer on the HOPG substrate, and its direction is indicative of the potential applied to the substrate relative to its potential of zero total charge (pztc). Given the flexibility of this technique, this finding also opens up possibilities to quickly probe the pztc of a material at the nanoscale under various experimental conditions. Once the meniscus is in contact with the substrate, discrete current steps were observed at potentials at which electrochemical reactions occur on Au but not on HOPG, indicating the arrival of distinct AuNPs. Three potential regimes can be distinguished: at potentials above 1 V (such as at 1.2 V, Figure 2a), the current steps are positive. At potentials below 0.15 V (Figure 2c and d), the current steps are negative, and the magnitude increases with more cathodic potential. Finally, at intermediate potentials (Figure 2b), no current steps are observed; instead the current-time profile shows a constant background. To understand this current-potential behavior in more detail, Figure 2e shows the

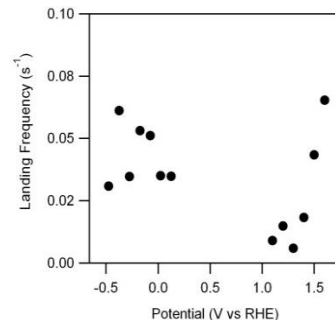


Figure 3: Frequency of current steps for landed NPs measured at different potentials.

mean values of the current steps as a function of substrate potential. There is a clear and strong potential dependence, similar to that of a bulk polycrystalline Au electrode measured using the same pipet setup (Figure 2f), although the current densities on the AuNPs are higher due to the much increased mass transport rate at nanostructures in the SECCM set-up.⁹ At low potentials (< 0.15 V), the observed current steps can be ascribed to the oxygen reduction reaction (ORR). The onset potential appears to be at a higher overpotential than on bulk Au (~ 0.4 V), but the apparent difference is likely due to the fact that the current steps at lower overpotential are not sufficiently large to be detected, although we also cannot rule out some kinetic effects at the smaller particle due to the greatly enhanced mass transport rate. At intermediate potentials, in the double layer region of Au, no current steps are observed, as no reaction takes place on the AuNP upon landing. This also indicates that the landing of NPs does not disturb the HOPG double layer significantly, while the charging of the particles themselves was not detected. Finally, at potentials positive of 1.10 V, oxidative current steps are observed. Typically, surface oxide formation takes place in this potential range. However, as this process is limited by the Au surface area, it would lead to current spikes with a finite charge (~ 5 fC for a 20 nm diameter AuNP)¹⁰, rather than current steps. As the oxidation of carbonaceous species is often found to take place in the Au surface oxidation region,¹¹ we tentatively attribute the oxidative current steps to the oxidation of residual carbonaceous species in solution, as no special effort was taken to purify the solution and reagents.

The excellent signal to noise ratio in these experiments allowed ready analysis of the frequency (number of current steps divided by the runtime of an experiment) at which AuNPs land on the HOPG substrate, as a function of the substrate potential (Figure 3). At the extreme potentials, the experimentally observed frequency is ~ 0.05 s⁻¹, lower than the theoretical value of 0.4 s⁻¹ predicted by diffusion laws¹² (see SI). Similar discrepancies have been consistently reported before.^{3c,d,13} Although various explanations have been forwarded to account for this discrepancy, the issue is not yet well understood. Finally, it should be noted that at moderately high potentials (between 1.0 and 1.5 V), the landing frequency lies below the average. As the magnitude of the current steps is very small in this potential region, we ascribe the diminished observed frequency to the fact that only particularly large or active particles show a catalytic response large enough to be detected, and thus the observed landing frequency may not represent the ‘true’ landing frequency.

A particularly exciting substrate on which to perform NP landing experiments is a transmission electron microscope (TEM) grid, as this allows characterization of the deposited NPs to fully resolve structure-activity relationships at the level of a single NP. To demonstrate this capability, we have landed AuNPs on a carbon coated TEM grid by measuring the oxidation of 2 mM hydrazine in a 50 mM citrate buffer. Although employing hydrazine with

citrate-capped NPs gave rise to some complications (*vide infra*), it is a good model system for an electrocatalytic reaction, as it is sufficiently facile to reach mass transport limited conditions. Typical landing events, in which the TEM grid was held at 1.25 V (potential close to the mass transport limited regime), are shown in Figure 4a. As can be seen, in these experiments, establishing the contact of the meniscus with the carbon film on the TEM grid typically coincides with the landing of the first AuNP, giving rise to current steps of $\sim 40 - 80$ pA. The magnitudes of these steps are in good agreement with the current predicted for the diffusion-limited current based on radial diffusion to a sphere with radius r on a plane, as given by equation 1.^{3a}

$$i_{\text{lim}} = 4\pi(\ln 2)nFDCr \quad (1)$$

Here n is the number of electrons transferred per hydrazine molecule (4), F is the Faraday constant (9.649×10^4 C mol⁻¹), C is the hydrazine concentration (2 $\mu\text{mol cm}^{-3}$), and D is the diffusion coefficient of hydrazine. A wide range of diffusion coefficients for hydrazine have been reported, typically $0.5 - 1.5 \times 10^{-5}$ cm² s⁻¹.¹⁴ In this case, we find the best correspondence between the spread in current step magnitudes and AuNP size distribution for $D \approx 1.2 \times 10^{-5}$ cm² s⁻¹, a value well within the reported range and typical for small molecules.

The landing frequency was low, with up to tens of seconds between successive landing events, attributable to a much lowered concentration of free AuNPs in solution due to extensive aggregation.¹³ This aggregation was observed qualitatively by the color change of a fairly concentrated AuNP solution upon addition of small amounts of hydrazine from pink to gray, followed by AuNP precipitation. Occasionally, these aggregates blocked the pipet completely, and no landings could be observed. In other cases, as Figure 4 shows, it is still possible to land single AuNPs without interference of aggregates landing, possibly due to the aggregates remaining mobile in solution, in which case the opening at the end of each barrel of the pipet (~ 700 nm) may act as a particle size filter. Furthermore, we cannot exclude other effects, such as the local interaction of the substrate with the AuNPs or the electrolyte solution, contributing to the lower landing frequency (compared to the HOPG substrate). Regardless, the long period between events allowed electrochemical characterization of the AuNP and then retraction of the pipet, leaving the initial AuNP on the TEM grid for subsequent visualization without further AuNPs landing. This makes it possible to correlate the electrochemical (current) with the physical properties of the AuNP. Examples are shown in Figure 4b: two separate landing experiments were performed with current steps of 40 and 60 pA. Visualizing these *same* particles with TEM, it can be seen that this difference is directly related to the size difference between the two AuNPs: the current step of 40 pA originating from a ~ 10 nm NP, while the current of 60 pA originates from a ~ 15 nm NP, in good agreement with equation (1). This agreement indicates directly that mass transport controls the reactivity of single AuNPs at

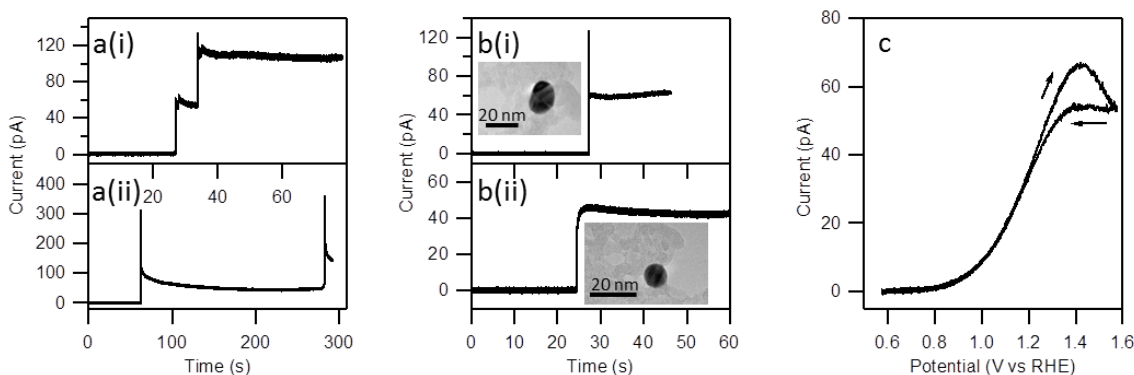


Figure 4 (a) AuNPs landing on a carbon coated Cu TEM grid (at 1.25V) in presence of N_2H_4 . (b) Landing events of individual AuNPs, with the *same* AuNP imaged by TEM afterwards. (c) CV (200 mV s^{-1}) measured at the individual AuNP shown in (b(i)).

this potential, and, moreover, the scaling of the current with particle radius confirms that mass transport to a single particle is predominantly radial in nature.

Finally, we were able to sweep the substrate potential after the initial landing event to record a full CV of a single AuNP before retracting the pipet. A CV of the AuNP in Figure 4b(i) is shown in Figure 4c. The recorded CV shows an onset potential of ~ 0.8 V, in good agreement with those reported for hydrazine oxidation on gold electrodes.¹⁵ The oxidation wave is somewhat drawn out compared to CVs recorded on macroscopic Au electrodes,¹⁵ which can be fully ascribed to the increased mass transport coefficient ($\sim 6\text{ cm s}^{-1}$, c.f. $\sim 10^{-3}\text{ cm s}^{-1}$ for macroscopic systems) in this configuration.⁸

In conclusion, we have demonstrated a SECCM-based approach to land and characterize single NPs on electrodes with minimal electrode preparation and the ability to select the measurement location. The results obtained with this approach are consistent with previous NP landing studies on UMEs^{3a-f} but with enhanced sensitivity due to the lower background signals owing to a smaller contact area. As highlighted herein, this pipet-based approach eliminates the need for UME fabrication, and a wide variety of substrates can be investigated. A particularly exciting application has been to use this pipet-based approach to study NP reactivity on a TEM grid, allowing the complete unambiguous correlation of physical and electrochemical properties at a single NP level for the first time. Apart from studying particle size and shape effects, the wide range of substrates that can be studied also opens up the possibility to study substrate effects on electrocatalytic reactions, an aspect which is not yet well-understood. We believe that these prospects make this pipet-based approach particularly powerful for further understanding and resolving nanoparticle reactivity.

ASSOCIATED CONTENT

Supporting Information

Experimental set-up, materials, AuNP synthesis, calculation of expected landing frequency. This material is available free of charge via the Internet at <http://pubs.acs.org>

AUTHOR INFORMATION

Corresponding Author

* m.koper@chem.leidenuniv.nl; p.r.unwin@warwick.ac.uk

Author Contributions

‡ These authors contributed equally.

ACKNOWLEDGMENT

We gratefully acknowledge Dr Alex Colburn and Mr Kim McKelvey for useful discussions and instrumentation design and

development. This work was supported by a Marie Curie Intra European Fellowship within FP7 of the European Community (no. 275450 “VISELCAT”) to SCSL, a European Research Council Advanced Investigator Grant (no. ERC-2009-AdG 247143 “QUANTIF”) to PRU, and the Netherlands Organisation for Scientific Research (NWO) through VIDI and VICI grants awarded to AIY and MTMK, respectively.

REFERENCES

- (1) (a) Somorjai, G. A. *Science* **1985**, *227*, 902; (b) Koper, M. T. M. *Nanoscale* **2011**, *3*, 2054; (c) Chen, A.; Holt-Hindle, P. *Chem. Rev.* **2010**, *110*, 3767.
- (2) Lai, S. C. S.; Dudin, P. V.; Macpherson, J. V.; Unwin, P. R. *J. Am. Chem. Soc.* **2011**, *133*, 10744.
- (3) (a) Xiao, X. Y.; Bard, A. J. *J. Am. Chem. Soc.* **2007**, *129*, 9610; (b) Bard, A. J.; Zhou, H.; Kwon, S. J. *Isr. J. Chem.* **2010**, *50*, 267; (c) Xiao, X.; Fan, F.-R. F.; Zhou, J.; Bard, A. J. *J. Am. Chem. Soc.* **2008**, *130*, 16669; (d) Zhou, Y.-G.; Rees, N. V.; Compton, R. G. *Angew. Chem.-Int. Edit.* **2011**, *50*, 4219; (e) Rees, N. V.; Zhou, Y.-G.; Compton, R. G. *RSC Adv.* **2012**, *2*, 379; (f) Kwon, S. J.; Bard, A. J. *J. Am. Chem. Soc.* **2012**, *134*, 7102; (g) Meier, J.; Friedrich, K. A.; Stimming, U. *Faraday Discuss.* **2002**, *121*, 365; (h) Chen, S.; Kucernak, A. *J. Phys. Chem. B* **2003**, *107*, 8392; (i) Krapf, D.; Wu, M.-Y.; Smeets, R. M. M.; Zandbergen, H. W.; Dekker, C.; Lemay, S. G. *Nano Lett.* **2005**, *6*, 105.
- (4) (a) Eikerling, M.; Meier, J.; Stimming, U. *Z. Phys. Chem.* **2003**, *217*, 395; (b) Hoeben, F. J. M.; Meijer, F. S.; Dekker, C.; Albracht, S. P. J.; Heering, H. A.; Lemay, S. G. *ACS Nano* **2008**, *2*, 2497.
- (5) (a) Kleijn, S. E. F.; Yanson, A. I.; Koper, M. T. M. *J. Electroanal. Chem.* **2012**, *666*, 19; (b) Li, Y. X.; Cox, J. T.; Zhang, B. *J. Am. Chem. Soc.* **2010**, *132*, 3047; (c) Cox, J. T.; Zhang, B. *Annu. Rev. Anal. Chem.* **2012**, *5*, 253.
- (6) (a) Frens, G. *Nat. Phys. Sci.* **1973**, *241*, 20; (b) Turkevich, J.; Stevenson, P. C.; Hillier, J. *Discuss. Faraday Soc.* **1951**, *11*, 55.
- (7) Snowden, M. E.; Güell, A. G.; Lai, S. C. S.; McKelvey, K.; Ebejer, N.; O’Connell, M. A.; Colburn, A. W.; Unwin, P. R. *Anal. Chem.* **2012**, *84*, 2483.
- (8) Lai, S. C. S.; Patel, A. N.; McKelvey, K.; Unwin, P. R. *Angew. Chem., Int. Ed.* **2012**, *51*, 5405.
- (9) Güell, A. G.; Ebejer, N.; Snowden, M. E.; McKelvey, K.; Macpherson, J. V.; Unwin, P. R. *Proc. Natl. Acad. Sci. U. S. A.* **2012**, *109*, 11487.
- (10) Angerstein-Kozłowska, H.; Conway, B. E.; Barnett, B.; Mozota, J. *J. Electroanal. Chem.* **1979**, *100*, 417.
- (11) Lai, S. C. S.; Kleijn, S. E. F.; Öztürk, F. T. Z.; Vellinga, V. C. V.; Koning, J.; Rodriguez, P.; Koper, M. T. M. *Catal. Today* **2010**, *154*, 92.
- (12) Bard, A. J.; Faulkner, L. R. *Electrochemical Methods: Fundamentals and Applications, 2nd Edition* **2001**.
- (13) Kleijn, S. E. F.; Serrano-Bou, B.; Yanson, A. I.; Koper, M. T. M. **2012**, Submitted.
- (14) (a) Zare, H. R.; Nasirizadeh, N. *Electrochim. Acta* **2007**, *52*, 4153; (b) Raoof, J.-B.; Ojani, R.; Mohammadpour, Z. *Int. J. Electrochem. Sci.* **2010**, *5*, 177; (c) Karp, S.; Meites, L. *J. Am. Chem. Soc.* **1962**, *84*, 906.
- (15) Alvarez-Ruiz, B.; Gomez, R.; Orts, J. M.; Feliu, J. M. *J. Electrochem. Soc.* **2002**, *149*, D35.

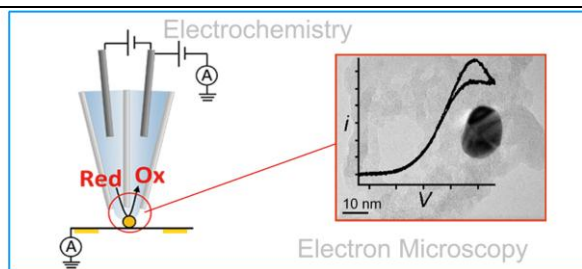


Table of Contents artwork